A new molar from the Middle Pleistocene hominid assemblage of Yanhuidong, Tongzi, South China

Anne Dambricourt Malassé, Pu Zhang, Patricia Wils

▶ **To cite this version:**

Anne Dambricourt Malassé, Pu Zhang, Patricia Wils. A new molar from the Middle Pleistocene hominid assemblage of Yanhuidong, Tongzi, South China. Acta Anthropologica Sinica, 2018, 37, pp.1 - 17. 10.16359/j.cnki.cn11-1963/q.2018.0001 . hal-02169687

HAL Id: hal-02169687
https://hal.science/hal-02169687

Submitted on 1 Jul 2019

HAL is a multi-disciplinary open access archive for the deposit and dissemination of scientific research documents, whether they are published or not. The documents may come from teaching and research institutions in France or abroad, or from public or private research centers.

L'archive ouverte pluridisciplinaire **HAL**, est destinée au dépôt et à la diffusion de documents scientifiques de niveau recherche, publiés ou non, émanant des établissements d'enseignement et de recherche français ou étrangers, des laboratoires publics ou privés.

DOI: 10.16359/j.cnki.cn11-1963/q.2018.0001

A new molar from the Middle Pleistocene hominid assemblage of Yanhuidong, Tongzi, South China

Anne DAMBRICOURT MALASSÉ[1], ZHANG Pu[2], Patricia WILS[3]

1. UMR 7194 CNRS National Museum of Natural History, Department of Man and Environment, Institute of Human Paleontology, 1 Rue René Panhard, 75013 Paris, France; 2. Guizhou Mountainous Resources Institute, Guizhou Academy of Sciences, 550001, Guiyang, Guizhou, China; 3. UMS 2700 CNRS-Muséum National d'Histoire Naturelle, 43, Rue Buffon, 75005 Paris, France

摘要：1988 年，贵州省博物馆对桐梓岩灰洞的支洞进行了最后一次发掘。2014 年，在洞内第四层堆积物中鉴定出逾 2000 件的动物牙齿化石，以及一枚古人类上颊齿（编号：TZ-1）。1991 年，铀系法测定这些次生堆积物的沉积年代约为距今 24 万年。本文运用高精度 CT（巴黎自然历史博物馆）对 TZ-1 的釉质齿质界面（EDJ）和牙髓腔几何形态进行了分析。TZ-1 的冠面形态有如下特征：次尖小且在远中舌侧不发育，咀嚼面轮廓呈四边形，颊舌径稍大过近中远中径，原尖舌侧齿带发育，齿尖从大到小依次为原尖、后尖、前尖和次尖。TZ-1 牙髓腔的髓角与其釉质齿质界面以及釉质表面的形态都具有相关性。TZ-1 的形态与 M^1 虽有相似之处，但完全不同于 1983 年出土于同一层位的另两颗 M^1；其应被鉴定为 dm^2，并可被归入中中更新世的中国直立人支系。岩灰洞上臼齿 PA 875 的形态与建始龙骨洞 PA 1279 和周口店直立人等古老型直立人相似。岩灰洞另一枚刚萌发的臼齿 PA 874 具有凸出的次尖和长菱形的外廓，接近于与爪哇型直立人 Sangiran NG 91-G10；这也是智人和尼安德特人的共有衍征。但 PA 874 的冠面仍保留了亚洲型的齿带，因而被归入人属未定种。因出土自次生堆积，岩灰洞的三种古人类类型未必曾同时并存，但却揭示了华南地区人类演化进程中的多样面貌。

关键词：桐梓；上颊齿；古人类；中国南方；中更新世

中图法分类号： Q983; **文献标识码** : A; **文章编号** : 1000-3193(2018)01-0001-17

Abstract：The last excavation of the small Yanhuidong gallery, Tongzi district, Guizhou Province, South China, was conducted by the Guizhou Provincial Museum in 1988. Fossiliferous layer IV of the endokarstic fill provided again more than 2,000 teeth with a new hominin upper molar referenced as TZ-1 in 2014. This secondary deposit has been dated 240 ka by Uranium Series in 1991. The description of the molar was completed by an analysis of the enamel-dentine junction (EDJ) and the topography of the pulp cavity using high-resolution µCT (v|tome|x L240-180) of the AST-RX platform, National Museum of Natural History, Paris, France. The crown

收稿日期：2017-06-27；　定稿日期：2017-12-12

基金项目：喀斯特高原山地旅游资源评价研究 (2016YFC0502606-002) ; UMR 7194/CNRS-National Museum of Natural History, Paris, France

作者简介：E-mail: anne.malasse@mnhn.fr

Citation: Dambricourt Malassé A, Zhang P, Wils P. A new molar in the Middle Pleistocene hominid assemblage of Yanhuidong, Tongzi, South China[J]. Acta Anthropologica Sinica, 2018, 37(1): 1-17

is characterized by a small hypocone without disto-lingual development, a trapezoidal shape of the occlusal contour, the bucco-lingual length slightly greater than the mesio-distal one, a large lingual cingulum on the protocone, and the cusps decrease in the order protocone, metacone, paracone and hypocone. The shape of the horns and of the bud horns from the pulp cavity are correlated with the morphology of the enamel-dentine junction (EDJ) and the outer enamel surface (OES). The tooth is a second primary molar (dm^2) assigned to a mid-Middle Pleistocene lineage of *H. erectus* living only in China (north-south axis Shanxi, Hubei, Hunan, Guandong and Guizhou provinces). The morphology that predicts M^1, does not match the two M^1 collected in 1983 in the same layer. PA 875 is close to the oldest pattern Jianshi PA 1279 also found at Zhoukoudian (Hebei and Hubei provinces). The germ PA 874 with its protruding hypocone and a rhomboidal shape is similar to the Javanese pattern Sangiran NG 91-G10; these are derived features shared in a certain way with *H. neanderthalensis,* but the crown keeps the Asian cingulum and is classified as *Homo incertae sedis*. These three morphological patterns are not necessary contemporaneous but they lift a veil on human settlements in South China before the redeposited faunal assemblage.

Key words: Tongzi; Deciduous molar; Hominin; South China; Middle Pleistocene

1 Introduction

The small Yanhuidong gallery (106°45' E, 28°75' N) was excavated in 1972 and 1983 by the Guizhou Provincial Museum in partnership with the Institute of Vertebrate Paleontology and Palaeoanthropology (I.V.P.P., Beijing).

The 190 cm-deep fill consists of seven layers of endokarstic flows, with Layer IV yielding more than 2,000 teeth, six of which were human, twelve stone tools, and traces of hearths (Fig.1). The animal assemblage was dated to the Middle Pleistocene and the six teeth attributed to *Homo erectus*[1] and later to Early *Homo sapiens*[2, 3]. The last excavation led by the Provincial Museum in 1988 emptied the fill and collected again more than 2,000 teeth presently housed at the Guiyang Academy of Sciences. An inventory list of animals was compiled in 1989[4], while a series of dating measurements was carried out by alpha spectrometry on eleven samples from speleothems[5]. Layer V is dated to 359^{+150}_{-6} ka BP, and Layer IV has been dated with two stalagmites embedded in this fossiliferous deposit. The first was fallen down while the second one was deposited on it. The results are respectively 257^{+42}_{-31} ka BP and 235^{+19}_{-16} ka BP. Since Layer IV is a secondary deposit, the age of the fossils goes back to the period between the two endokarstic flows (Layers V and IV) but the species with more than 4,000 teeth and rare bones, were not necessary contemporaneous. Nevertheless the fauna indicates a hot, humid sub-tropical climate with meadows and forest landscapes.

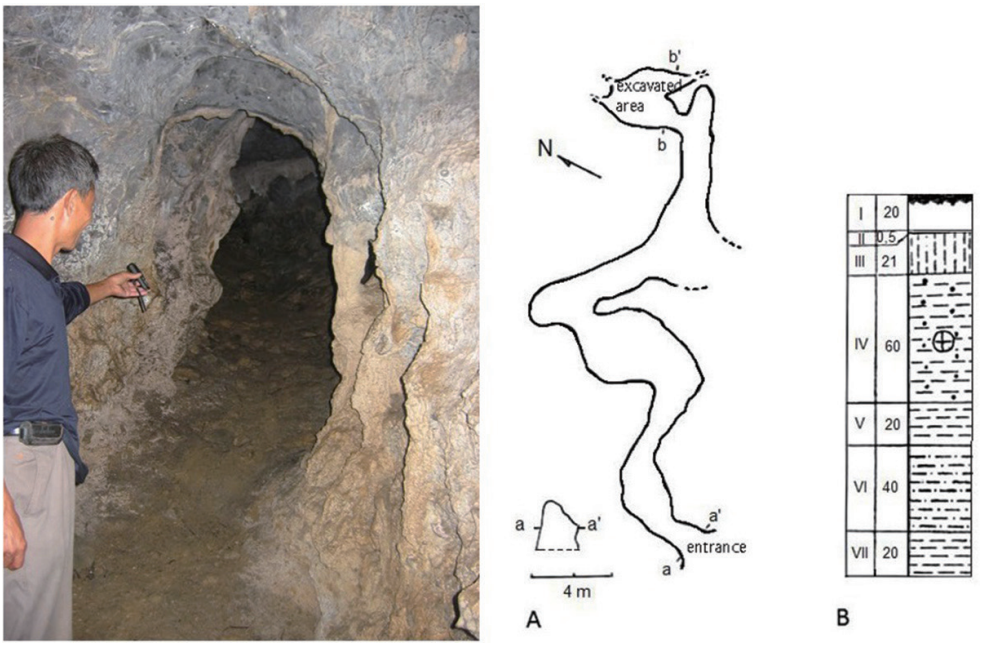

Fig.1 The Yanhuidong gallery and the profile with the excavation (A) and the lithostratigraphy (B) of the section b-b'. Layer IV is the fossiliferous deposit with a cross in a circle (after Wu et al., 1975, picture A. Dambricourt Malassé)

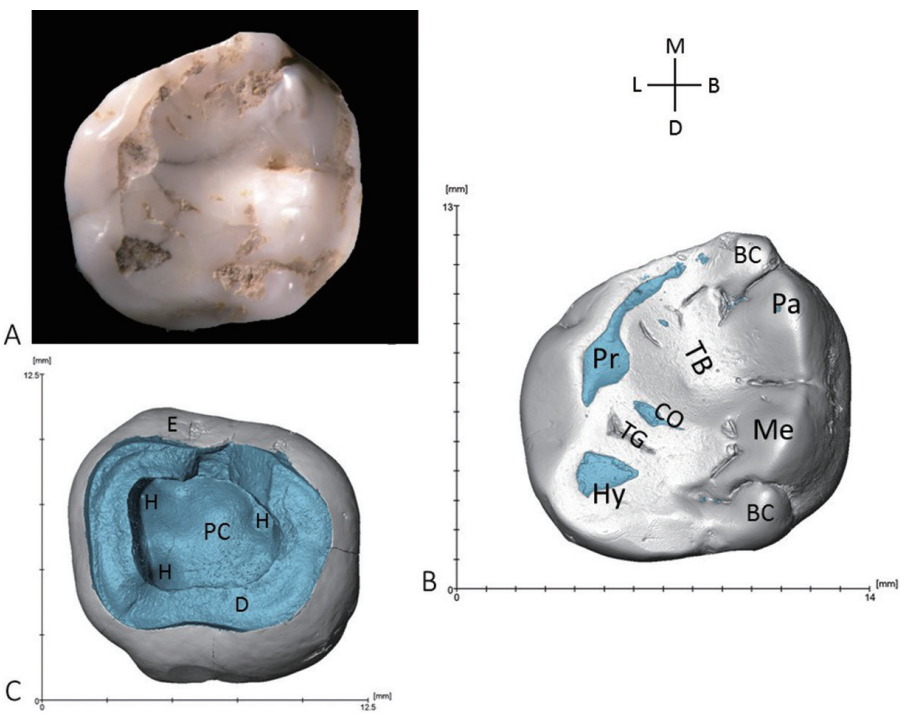

Fig.2 Upper molar from Yanhuidong, TZ-1. A: occlusal view of the original molar, B: high-resolution µCT in occlusal view, C: high-resolution µCT in inferior view. BC: buccal cusplet, CO: crista obliqua, D: dentine, E: enamel, H: horn of the dentine, Hy: hypocone, Me: metacone, Pa: paracone, PC: pulp cavity, Pr: protocone, TB: trigonid basin, TG: talonid groove

The list of fauna and the study of the collection resumed in 2009 and were published with a preliminary description of the new molar allocated to a *Homo erectus* pattern[4]. We present here a morphological and metric study with a description of the enamel-dentine junction (EDJ), the topography of the pulp cavity and their relations with the outer enamel surface (OES), using the high-resolution μCT (v|tome|x L240-180) of the AST-RX platform of the National Museum of Natural History, Paris. Then we compare the outer enamel morphology with two others M^1 from Tongzi, fossil species of *Homo* and *Homo sapiens*. In this study, *Homo sapiens* Linné 1758, corresponds to the more straightened neural system with the cerebellar fossa in a more forward position[6, 7].

2 Human teeth

2.1 Material and methods

The second primary molar is exceptionally preserved in the Lower and Middle Pleistocene fossil records with two isolated dm^2 reported, Tighenif (Ternifine, Algeria, 700 ka)[8] similar to *Homo sapiens* and allocated to *H. heidelbergensis*[9] and Sangiran 7-13 (Indonesia, 700 ka) "classified ambiguously" after its crown outline shape has been compared with *Homo sapiens* and *Homo neanderthalensis*[10]. The lack of Chinese specimen can be solved by the comparison with M^1 because 1) the dm^2 keeps more conservative external crown morphology than does M^1 [11] and 2) the tooth germ of dm^2 and M^1 share the same prenatal growth pattern[12]. Since the TZ-1 tooth is very probably dm^2, the comparison with a large sample of fossil and modern M^1 helps to identify its lineage.

The data used for comparison were collected from 107 fossils: 23 originals, 27 high-resolution casts from the collections of the Institute of Human Palaeontology, Paris (IPH), and 57 specimen reported in the scientific literature (Tab.1 and Tab.2). Fossil casts lend support to the published data collected with new technique (geometrical morphometry, X-ray microtomography) and that sets the criteria to identify plesiomorphic patterns and derived morphologies[e.g. 13 to 28].

Volumetric differences of the cusps alter the shape of the tooth in occlusal view[27]. These differences are measured by X-ray microtomography[20, 21] or by geometrical morphometry[26, 27, 28]. The hypocone bulges lingually and distally in *H. antecessor* and in *Homo sapiens* (AMH) giving the crown a rhomboidal shape. The rhomboidal profile is also one of *H. heidelbergensis* and is pronounced in *H. neanderthalensis* because of a protruding hypocone[26]. By contrast, one pattern of East Asian M^1 is the low development of the hypocone on the disto-lingual side, and of the paracone on the mesio-buccal side, giving a trapezoidal shape to the outline of the crown[27].

2.2 Molars PA 874 and PA 875 from the 1983 excavation

The dental collection is housed at IVPP, Beijing. The teeth have been previously described and compared to a series of Asian fossil hominins[33, 34]. We recall the description of two M^1, and complete them with our observations.

PA 874 (Fig.3A) is a first left upper molar with growing roots. The cervix is convex on all sides, the cingulum is especially developed buccally. The virtual polygone connecting the tip of the cusps draws a rhombus. On the occlusal surface, the groove between the hypocone and protocone joins the lingual groove. The longest bucco-lingual length of the crown is 11.1 mm, and the mesio-distal one, 10.5 mm. Its proportions are smaller than Zhoukoudian, Hexian (PA 836), and Xichuan (PA 529). The tooth has been attributed to a young *Homo erectus* aged 6 years.

We note the absence of wear on the occlusal surface and lack of interproximal wear facet. PA 874 is a tooth germ. The germ differs from SKD 140 (cast, Zhoukoudian locality, 750 ka to 400 ka BP[35]) by the absence of a cingulum on the lingual side of the protocone, a large disto-lingual development of the hypocone and a paracone distinctly more pronounced than the metacone. The distal edge is complicated by an accessory cusp (metaconule or cusp 5). The distance between the tips of the paracone and hypocone is clearly longer than between the protocone and metacone. Consequently, the crown outline shape is rhomboidal.

PA 875 (Fig.3B) is a right upper molar, M^1 rather than M^2. The longest bucco-lingual length of the crown is 14 mm, and the mesio-distal length 11.4 mm. The position of the sulcus sagittalis is median, comparable to Zhoukoudian. The robust roots are partially preserved on the buccal side, and are complete on the lingual side. Wu[33] has also noted their bucco-lingual gap wider than the one in *Homo sapiens* and *Homo neanderthalensis*. These traits conform closely to the teeth of Zhoukoudian and are characteristic of *Homo erectus* variability.

Our observation provides some details: the sulcus sagittalis is not palpable but the crista obliqua is visible between the protocone and metacone. The occlusal surface is worn down to the dentine of the protocone but only slightly on the hypocone, corresponding to Molnar Stage 3[36]. The metacone is substantially bigger than the paracone, the crown shape is rectangular, the surfaces of the protocone and hypocone are developed, but this last feature does not shape a protruding cone. The lingual cingulum is poorly developed, contact facets are well marked, and the bucco-lingual gap between the roots is not as broad as ZKD 33 (cast). However, the shapes of the crown outline are similar.

To resume, PA 874 is a germ with a cingulum on the buccal side but rather low on the protocone. The crown distinguishes itself by the rhomboidal shape due to a protruding hypocone and a paracone larger than the metacone. PA 875 has not the same lustrous appearance, the tooth is larger and the protocone has no cingulum on the lingual surface.

2.3 TZ-1molar from 1988 excavation

2.3.1 The crown morphology

The crown is preserved but the roots are destroyed (Fig.2C, Fig.4) like for most teeth of Layer IV. The enamel is lustrous with marbled appearance. On the occlusal surface, the paracone and metacone adjoin a small buccal accessory cone (cusplet) well-separated by a groove and which cannot be confused with the mesial and distal cusplets (Fig.2B). The protocone and hypocone are worn and expose the dentine, this wear corresponds to Molnar Stage 4. The sulcus sagittalis is no more visible in the trigonid basin but the crista obliqua is still discernible, as well as the groove between the crista obliqua and hypocone.

The contact facet of the distal side is small with two contiguous asymmetrical circular surfaces (Fig.4D). On the mesial side, the facet is higher and wider, rectangular in shape, with rounded lingual and buccal edges (Fig.4C). The lingual surface of the protocone features a well-developed cingulum with a short vertical groove (mesio-lingual groove) separating it from the mesial marginal ridge (Fig.4B and 4C).

The bucco-lingual section viewed by X-ray microtomography presents evenly shaped enamel that rules out a Carabelli tubercle (Fig.5A). The cervix visible from the buccal side (Fig.4A) is also curved on the mesial face and not rectilinear as dm^2 or M^1 in *Homo sapiens*. The hypocone is not disto-lingually developed, and the curve on the buccal side between the two accessory cones is longer and less convex than its lingual counterpart. The shape of the crown outline is trapezoidal.

2.3.2 Dentine morphology

Topography of the enamel-dentine junction (EDJ) and the pulp cavity

Occlusal view of the EDJ

The topography of the EDJ is consistent with the outer occlusal surface (Fig.5). On the buccal side, the dentine horns of the paracone and metacone are well visible with that of their respective cusplets. On the lingual side, the protocone and hypocone dentine are apparent on the occlusal face, their plane surfaces are connected by a crest separating the distal fovea and the depression equivalent to the disto-lingual groove. The dentine is also visible on the crista obliqua and corresponds to the horn of an accessory cusplet of this ridge (Fig.5). Two small horns are visible between the protocone and paracone, in the trigone basin (or central fossa) below the surface of the enamel. The EDJ ridge joining the protocone to the cusplet of the metacone shows three eroded denticules of dentine (Fig.5).

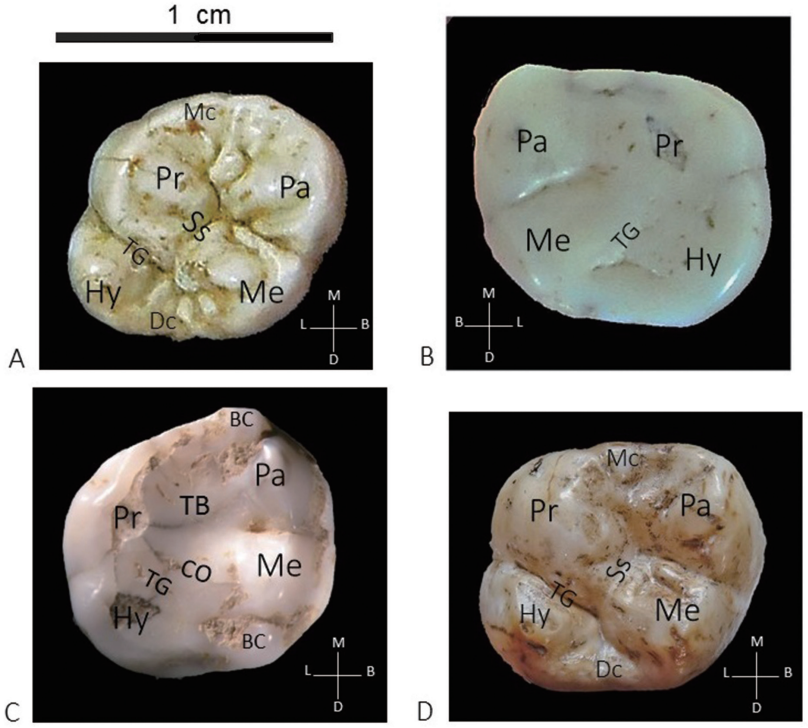

Fig.3 Morphological comparison between PA 874 (A), PA 875 (B), TZ-1 (C) and left M1 of Qafzeh 4 (D)

CO: crista obliqua, Dc: distal cusplet (metaconule or cusp 5), Hy: hypocone, Mc: mesial marginal tubercle, Me: metacone, Pa: paracone, Pr: protocone, Ss: sulcus sagittalis, TG: talonid groove. Pictures of PA 874 and PA 875, courtesy from Wu Xinzhi and Cui Yamei. Pictures of TZ-1 and Qafzeh 4, A. Dambricourt Malassé

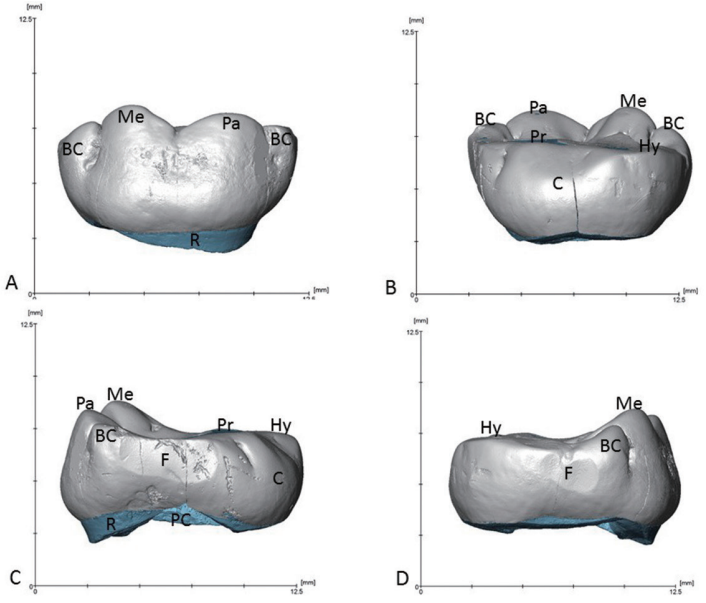

Fig.4 High resolution µCT of TZ-1, lateral views, A: buccal, B: lingual, C: mesial, D: distal. BC: buccal cusplet, C: cingulum, F: contact facet, Hy: hypocone, Me: metacone, Pa: paracone, PC: pulp cavity, Pr: protocone, R: root

Sectional views of the EDJ and internal observations of the crown

The pulp cavity forms the internal topography of the dentine (Fig.6).

On the lingual side, the pulp cavity presents two plateaus (or horn buds) below the occlusal surface of the protocone and hypocone (Fig.6A). The foot of the pulp cavity is slightly bulged, but the dentine thickens towards the lingual side, forming a bulge with the EDJ. The curvature of the EDJ extends occlusally, then inflects buccally at the level of the ceiling of the pulp cavity (Fig.6A, 1). The EDJ curvature inflects a second time (Fig.6A, 2), and straightens out up to the occlusal surface, where enamel is worn away. The growth of the enamel has not followed these variations. The external curvature of the enamel, which begins at the cervix, extends evenly up to the occlusal surface. This regular feature is reflected by a thickening of the enamel that compensates for the second inflection of the EDJ's curvature. This thickening results in the formation of the cingulum, which is maximal as the approach of the occlusal surface (Fig.6A, 6B).

On the buccal side, the foot of the pulp cavity is slightly symmetrical with one on the lingual side (Fig.6A). It starts vertically, the dentine thickens buccally and forms a bulge clearly visible, then, the dentine bulge ends at the level of the pulp cavity's ceiling (Fig.6A : 1'), but the EDJ evens out more vertically than its lingual homologue (Fig.6: 2'). Before slanting horizontally beneath the occlusal surface, the EDJ forms a crest whose height varies mesio-distally. The maximum height of the dentine is measured between the tip of a pulp horn and that of the dentine horn: 2.63 mm for the paracone and 2.68 mm for the metacone (Fig.6C and Fig.6D). We note a relationship between enamel thickness, the variations of the

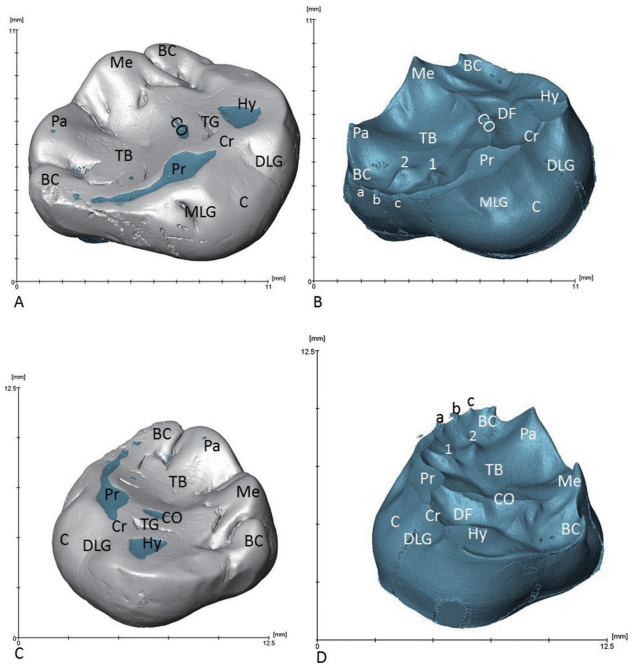

Fig.5 High resolution µCT of TZ-1, comparison between the outer surface enamel and the enamel-dentine junction (EDJ). High: mesio-lingual viewing angle; Low: disto-lingual viewing angle. BC: buccal cusplet, C: cingulum, CO: crista obliqua, Cr: edge between the protocone and the hypocone, DF: distal fovea, DLG: disto-lingual groove, Hy: hypocone, Me: metacone, MLG: mesio-lingual groove, Pa: paracone, Pr: protocone, TB: trigonid basin, TG: talonid groove; 1, 2, small dentine horns of accessory cusplets in the trigonid basin; a,b,c, small horns of mesial accessory tubercles

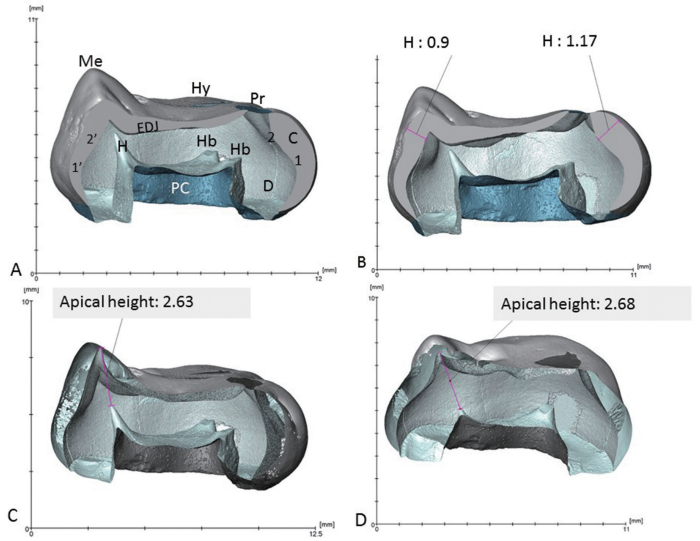

Fig.6 High resolution µCT of TZ-1, frontal section crossing the protocone and the metacone, A: anatomical description, B: maximum high of the enamel of the two cones at this section, C: maximal high of the paracone dentine horn. C: cingulum, D: dentine, EDJ: enamel dentine junction, H: horn, Hb: horn bud, Hy: hypocone, Me: metacone, PC pulp chamber, Pr: protocone, 1, 1', 2, 2': inflection points of the EDJ. Measurements are in millimetres

EDJ curvatures and the presence or absence of a pulp horn. Under the paracone, the pulp cavity forms a long oblique horn directed buccally. Under the metacone, the horn is very short, while there are only two plateaux on the lingual side.

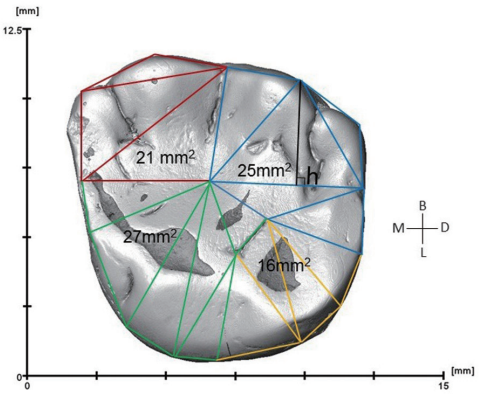

Fig.7 Calculation of the surfaces of the four cusps with the method of the right-angle triangle (s=base x h/2). The base of each triangle and their height (h) have been measured on the microtomography (green: protocone, red : paracone; blue : metacone and yellow : hypocone)

The maximum thickness of the paracone enamel can be seen on the buccal and not on the occlusal side, probably due to wear. But, on the same cross-section, the maximum thickness of the enamel is 1.17 mm for the protocone and 0.9 mm for the paracone (Fig.6B). This difference reflects the asymmetrical curvature of the EDJ caused by the horns and the plateaus of the pulp cavity. Indeed, under the paracone the EDJ curvature becomes vertical sooner than under the protocone, as deflected by the dip of the large pulp horn, while there is none on the lingual side where the enamel become thicker with the cingulum. The same principle can be seen with the metacone.

Tab.1 Largest dimensions in millimetre of M^1 and dm^2 since the Lower Pleistocene.
Specimen are originals (*), casts or from authors. MD: mesio-buccal, BL: bucco-lingual

Specimen	Age	Locality	Taxon	dm^2		M^1	
				MD	BL	MD	BL
China							
Sinanthropus[34] male (*n*=1)	early Mid- Pleistocene	Zhoukoudian	*erectus*	-	-	12.6	13.4
Sinanthropus[34] female (*n*=5)	early Mid- Pleistocene	Zhoukoudian	*erectus*	-	-	10.6	12.4
PA 529[34] M^1 or M^2	No context	Xichuan	*erectus*	-	-	12.7	14.8
PA 530[34] M^1 or M^2	No context	Xichuan	*erectus*	-	-	12.6	14.3
PA 637[34]	No dating	Yunxian (Meipu)	*erectus*	-	-	12.9	13.9
Chaoxian [16]	360-310 ka	Chaoxian	*erectus*	-	-	11.7	13.5
PA 874*	>240 ka	Tongzi	*incertidae sedis.*	-	-	10.5	11.1
PA 875*	>240 ka	Tongzi	*erectus*	-	-	11.4	14
TZ-1*	>240 ka	Tongzi	*erectus*	10.3	11.1	-	-
PA 1480-5 [22]	early Late Pleistocene	Xujiayao	*erectus*	-	-	13.4	14
PA 1496 [22]	early Late Pleistocene	Xujiayao	*erectus*	-	-	11.5	13.2
Changyang[33]	195 ka	Changyang	*erectus*	-	-	10.8	12.8
PA 836 [34]	190-150 ka	Hexian	*erectus*	-	-	12.3	13.7
China[33]	actual	China	*sapiens*	-	-	10.1	11.3
Other Asian localities							
Sangiran[15] (*n*=2) Pucangan, Kabuh	1.8 Ma & 0.8 ka	Indonesia	*erectus*	-	-	12.1	13.1
Dmanisi (*n*=2) [14]	1.8 Ma	Georgia	*georgicus*	-	-	12.7	12.9
Qafzeh 3*	95 ka	Israel	*sapiens*	-	-	11.1	11.1
Qafzeh 4*	95 ka	Israel	*sapiens*	9	9	11	11
Qafzeh 5*	95 ka	Israel	*sapiens*	-	-	11	11
Qafzeh 7*	95 ka	Israel	*sapiens*	-	-	12	13
AMH (*n*=300)[11]	actual	Japan	*sapiens*	8.6	9.7	-	-
AMH (*n*=200)[32]	actual	India	*sapiens*	-	-	10.1	10.6
Africa							
Tighenif [8]	700 ka	Algeria	*heidelberg.*[9]	10.2	11.8	-	-
Rabat cast	370 ka	Morocco	*ergaster*[26]	-	-	12	12
Irhoud 10[55]	300 ka	Morocco	*sapiens*	-	-	12.1	12.2
Irhoud 21[55]	300 ka	Morocco	*sapiens*	-	-	12.2	12.7
Afalou 17*	15-11 ka	Algeria	*sapiens*	10	10	11	12
Afalou 19*	15-11 ka	Algeria	*sapiens*	10	10	-	-
Taforalt XVI*	12-10 ka	Morocco	*sapiens*	9	10	-	-
Taforalt 1968-1*	12-10 ka	Morocco	*sapiens*	10	10	-	-
Redeyef*	Neolithic	Tunisia	*sapiens*	10	9	-	-
Europe							
Pontnewydd PN 4[30]	225 ka	England	*neand.*	9.8	10.3	12.2	12.4
Krapina [37] (*n*=10)	130	Croatia	*neand.*	10.3	10.7	-	-
Neandertal [8] (*n*=8)	Upper Pleistocene	Eurasia	*neand.*	9.3	10.2	-	-
Pech de l'Azé cast	51-41 ka	France	*neand.*	10	10	-	-
Grotta de Cavallo [31]	45-43 ka	Italy	*sapiens*	10	11	-	-
La Genière cast	Mesolithic	France	*sapiens*	9	9	-	-
Bennac* (*n*=10)	Chalcolithic	France	*sapiens*	-	-	9.8	10.9

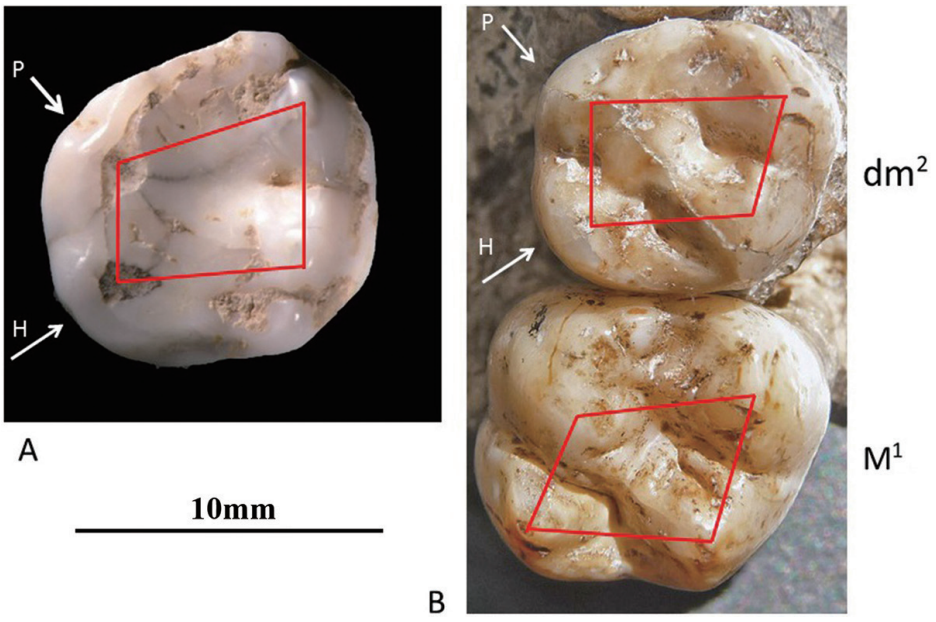

Fig.8 Comparison between TZ-1 (A), dm^2 and M^1 of Qafzeh 4 (B). The polygon between the four cusps illustrates the trapezoidal (A) and rhomboidal (B) organization. H: hypocone, P: protocone (original teeth, picture A. Dambricourt Malassé)

2.3.3 Size and measurements

The relative proportion for each cusp is calculated by the conventional method of a right-angle triangle applied on the microtomography, this image is the projection of the crown on the horizontal plane (Fig.7). The hypocone is circumscribed by the talonid groove, the disto-lingual groove and the weak depression between two small peaks on the distal edge. The limit between the protocone and metacone is the line joining the lower points of the crista obliqua and of the trigonid basin, and the one between the protocone and the paracone is drawn from this point to the most incurved point of the mesial edge. The projected areas decrease from the protocone ($27mm^2$) to the metacone ($25mm^2$) substantially greater than the paracone ($21\ mm^2$) and finally to the hypocone ($16mm^2$).

The largest dimensions of the occlusal surface measured by microtomography are 11.1 mm for the bucco-lingual length and 10.3 mm for the mesio-distal length. The maximum height of the crown is 7 mm at the paracone. The measures of a significant sample of dm^2 and M^1 allow us to discriminate the type of molar (Tab.1). According to[22], identifying Pleistocene taxon in China become complex because of unknown lineages, nevertheless we keep the name *erectus* when the tooth cannot be confused with AMH and *Homo neanderthalensis*.

The maximal bucco-lingual and mesio-distal dimensions of TZ-1 are similar to the germ PA 874 but the contour of the crown and development of the cusp are different. The shape of TZ-1 is

Tab.2 M^1 and dm^2 crown outline shape (COS) of *Homo* since Lower Pleistocene

Note: Specimen are originals (*), casts or from good quality pictures with their references. L: left, R: right

	Specimen	Age	Region	species	M^1	dm^2	COS
China	Jianshi PA 1279 [28,29]	≥ 2.15 Ma	Hubei	*erectus*	L		rectangular
	Zhoukoudian loc.O n°1	750-670 ka	Hebei	*erectus*	L		rectangular
	Zhoukoudian ZKD 140	750-670 ka	Hebei	*erectus*	L		rectangular
	Zhoukoudian ZKD 33	750-670 ka	Hebei	*erectus*	L		rectangular
	Hexian PA 836[21]	412 ka	Anhui	*erectus*	L		sub-square
	Chaoxian[16]	410 ka	Anhui	*erectus*	L R		rectangular
	Xujiayao PA1496 [22,50]	370-260 ka	Shanxi	*erectus*	L		trapezoidal
	Xujiayao PA1480-5[22,50]	370-260 ka	Shanxi	*erectus*	L		trapezoidal
	Tongzi PA 875*	≥ 240 ka	Guizhou	*erectus*	R		rectangular
	Tongzi TZ-1*	≥ 240 ka	Guizhou	*erectus*	L		trapezoidal
	Tongzi PA 874*	≥ 240 ka	Guizhou	*sp. incert.*	L		rhomboidal
	PA 637 [34] Meipu	No dating	Hubei	*erectus*	L		rhomboidal
	Changyang [38]	195 ka	Hubei	*erectus*	L		trapezoidal
	Shuidong-Maba 3 [39, 48]	uncertain	Guandong	*erectus*	R		trapezoidal
	Shuidong-Maba 4 [39, 48]	uncertain	Guandong	*sapiens*	R		rhomboidal
	Daoxian DX 36-o [51,52]	uncertain	Hunan	*erectus*	L		trapezoidal
	Daoxian DX 1-o [51,52]	uncertain	Hunan	*sapiens*	L		rhomboidal
	Daoxian DX 28-o [51,52]	uncertain	Hunan	*sapiens*	L		rhomboidal
Southeast Asia	SangiranBPG2001-04[53]	1.5 Ma	Indonesia	*erectus*	L		square
	SangiranNG 91G10-1[20]	790 ka	Indonesia	*erectus*	L		rhomboidal
	Sangiran 17	500 ka	Indonesia	*erectus*			square
	Tam Pong*	Mesolithic	Laos	*sapiens*	L R		rhomboidal
Central Asia	Teshik Tash	Middle Paleolithic	Ouzbekistan	*neandert.*	L R		derived rhomboidal
Western Asia	Dmanisi 2700[14] and cast	1.8 Ma	Georgia	*georgicus*	R		square
	Skhul IV	130-100 ka	Israel	*sapiens*	L		rhomboidal
	Skhul V	130-100 ka	Israel	*sapiens*	L R		rhomboidal
	Qafzeh 3*	120 - 90 ka	Israel	*sapiens*	L		rhomboidal
	Qafzeh 4*	120 - 90 ka	Israel	*sapiens*	L	L	rhomboidal
	Qafzeh 5*	120 - 90 ka	Israel	*sapiens*	L R		rhomboidal
	Qafzeh 7*	120 - 90 ka	Israel	*sapiens*	L R		rhomboidal
Africa	Ishango [42]	≥ 2 Ma	Congo	Australopith or Early *Homo*	L		square
	KNMER 62000 [43]	1.95-1.91 Ma	Kenya	Early *Homo*	L		square
	OH 24	1.8 Ma	Tanzania	*habilis*	L		square
	KNMER 3733	1.7 Ma	Kenya	*ergaster*	L R		square
	KNMER 15000	1.6 Ma	Kenya	*ergaster*	L R		square
	Cornelia-Uitzoek [44] COR 2011	1.07-0.99 Ma	South Africa	*sp. incert.*	R		rhomboidal
	Tighenif [8,9]	700 ka	Algeria	*heidelberg.*			rhomboidal
	Rabat	370 ka	Morocco	*ergaster* [26]	L		square

Tab.2 M^1 and dm^2 crown outline shape (COS) of *Homo* since Lower Pleistocene (Continued)

Note: Specimen are originals (*), casts or from good quality pictures with their references. L: left, R: right

	Specimen	Age	Region	species	M^1	dm^2	COS
	Irhoud 10 [54, 55]	300 ka	Morocco	*sapiens* (?)	L		square
	Dinaledi H1 [45, 46]	250 ka	South Africa	*naledi*	L		rhomboidal
	Herto [47]	160-154 ka	Ethiopia	*sapiens*	L R		rhomboidal
Europe	Atapuerca ATD 6-69	1.2 Ma -700 ka	Spain	*antecessor*	L R		rhomboidal
	Arago XXI	450-300 ka	France	*heidelberg.*	L		slightly rhomboidal
	Petralona	350-150 ka	Greece	*heidelberg.*	L R		rhomboidal
	La Quina H18	75-45 ka	France	*neandert.*	L R		derived rhomboidal
	La Quina H5	75-45 ka	France	*neandert*	L		derived rhomboidal
	Le Moustier	56-40 ka	France	*neandert*	L R		derived rhomboidal
	Le Pech de l'Azé	51-41 ka	France	*neandert*	L R		derived rhomboidal
	Bennac* (*n*=10)	Chalcolithic	France	*sapiens*	L		rhomboidal

trapezoidal because of a lesser development of the protocone, whereas the rhomboidal shape of PA 874 is due to the protrusive disto-lingual development of the hypocone and the mesio-buccal development of the paracone (Fig.3). Accordingly, TZ-1 and PA 874 developed two different growth patterns. TZ-1 is smaller than PA 875, but the pattern are not similar as the bulge of the crown forms a constriction all around the cervix of TZ-1 (Fig.4) and this feature is missing on PA 875. Moreover such a cingulum does not match the constriction of the AMH dm^2 restricted to the hypocone and less pronounced. On the other hand, the generalization of the cingulum to the crown is visible at Zhoukoudian with S36 (left M^1) and S40 (right M^2), and characterizes an ontogenetic pattern of *Homo erectus* that should be the same for dm^2. The size of TZ-1 is smaller than M^1 whatever the Early and Middle Pleistocene Asian localities.

By comparison with other dm^2, the dimensions of TZ-1 are smaller than *H.heidelbergensis* (Tighenif), slightly greater than early and robust *Homo sapiens* (Qafzeh-early Late Pleistocene, and Afalou-Taforalt-Late Pleistocene) and greater than gracile *Homo sapiens* (Neolithic-actual). The surface of the cusps decreases according to the plesiomorphic pattern in the order protocone, metacone, paracone, and hypocone. Ultimately, the pre-natal growth pattern of TZ-1 is plesiomorphic with an Asian *H. erectus* trait characterized by the cingulum, this odontogenesis differs from *H. heidelbergensis*, *H. sapiens* and *H. neanderthalensis*. To conclude and despite the lack of homologous tooth for demonstration, the low height and occlusal dimensions of the crown assigned TZ-1 to a second temporary molar from an Asian *Homo erectus* lineage, with a growth pattern different from PA 874 and PA 875.

2.3.4 Comparison of outer enamel surfaces (OES) and crown outline shapes (COS)

No comparison between dm^2 and M^1 from the same *Homo erectus* specimen is possible in order to identify the lineage of TZ-1, nevertheless the comparison between its COS with others M^1

allows a first approximation. The crown outline shape of M^1 is useful for taxonomical distinction, especially for the rhomboidal pattern between *Homo antecessor,* European and African *H. heidelbergensis*, *H. sapiens* and the derived shape *H. neanderthalensis* due to a very protruding hypocone[17]. For clarity of analysis this last contour is called "derived rhomboidal".

The outer enamel surfaces (OES) and crown outline shapes (COS) of dm^2 is well known in early and modern *Homo sapiens* with a rhomboidal contour such as Qafzeh 4 (Fig.8) and Grotta del Cavallo[31, fig.3], this profile was already visible with a North-African *H. heidelbergensis*[10]. The COS of TZ-1 shows a pronounced trapezoidal shape due to the lower development of the hypocone and of the protocone (Fig.8). Comparisons in Tab.2 assign TZ-1 to a Chinese *H. erectus* lineage.

The lingual cingulum visible on TZ-1 is missing on the oldest M^1 collected in China, Jianshi PA 1279[fig.9a in 28]. On the contrary, the cingulum is distinctly apparent on the lingual and buccal surfaces of Zhoukoudian ZKD 140 and on the Javanese molar Trinil 1620 (M^1 or M^2) attributed to *Homo erectus*[fig.1 and fig.2 in 15].

The cones decrease in the plesiomorphic order in *Homo georgicus* D 2700 and the hypocone does not project disto-lingually, nevertheless the occlusal contour is square-shaped because of a small c5 cuspid on the distal edge. The COS of TZ-1 does not conform to *Homo georgicus*.

TZ-1 does not conform to the rectangular-shaped Jianshi PA 1279, ZKD Loc.1, ZKD 33, ZKD 140 and Chaoxian[fig.2c in 16 and original picture]. The trapezoidal shape brings TZ-1 closer Xujiayao PA1480 "square-shaped with a slight disto-buccal constriction" and PA1496[fig.1 and fig.3 in 22], Changyang and the M^1 of Shuidong with the roots[fig.3 C5 in 39]. The second rootless M^1 from Shuidong is rhomboidal with prominent paracone and hypocone[fig.3 D5 in 39]. Finally TZ-1 cannot be confused with any Asian specimen outside China: Sangiran BPG 2001-04[fig.3 in 53] and Sangiran 17 (Java) are rectangular, Sangiran NG 91-G10[fig.S3 in 20] is rhomboidal, the hypocone of *Homo floresiensis* has no disto-lingual prominence, however, the crown is rectangular-shaped, mesio-distally very narrow, and presents no cingulum[fig.1C in 40].

3 Discussion and conclusion

Tab.2 shows a first distinction between African (square-shaped COS) and Chinese fossils (rectangular and trapezoidal shaped COS). PA 875 matches the oldest M^1 pattern of Jianshi PA 1279 (2.15-1.95 Ma) with its rectangular shape and lack of cingulum; this pattern is found again at Zhoukoudian and appears nowhere else in Africa, Europe and Asia. The trapezoidal contour of TZ-1 could match a Chinese lineage observed since the mid-Middle Pleistocene from north to south China (Shanxi, Hubei, Hunan and Guizhou provinces) and possibly during

the Upper Pleistocene (Shuidong and Guandong provinces)[49]. This hypothesis supports a regional lineage deduced from Xujiayao[22].

PA 874 delivers a second distinction between African and Asian molars with a derived rhomboidal shape and explains the new attribution to early *Homo sapiens*[3]. Nevertheless the tooth is dated at least to 240 ka and the rhomboidal contour is more derived than *Homo sapiens* Qafzeh 4 (Fig.3). The rhomboidal outline dates back at least one million years in South Africa with *Homo sp*. from Cornelia-Uitzoek (1.01 Ma-0.9 Ma)[44] and is found again in South Africa with the M^1 series of *Homo naledi*[200 ka, 45], (fig.1 in 46). The rhomboidal shape was visible in Western Europe during the same period with a slightly protruding hypocone in *Homo antecessor* (1.2 Ma-0.7 Ma). The derived rhomboidal shape was visible in South East Asia at 700 ka with NG91-G10 (Java) and PA 874 is more derived than the Javanese molar. So we can deduce that a trend similar to the one from *H. heidelbergensis* to *H. neanderthalensis* was visible in South Asia during the Lower and Middle Pleistocene. No early *H. sapiens* is evidenced in the Yanhuidong assemblage, but PA 874 is closer to the common ancestor with AMH than Jebel Irhoud 10 (Morocco) dated back 300 ka[54]. The isolated maxillary is claimed as the oldest specimen of a pan-African archaic *Homo sapiens* grade[55] nevertheless high-tech analysis of the M^1 crown outline[fig.1 and extended data fig.2 in 55] indicates a squared-shape more pronounced than Rabat (Morocco, 370 ka) classified as *H. ergaster*[26].

To conclude, the upper molars of Yanhuidong recorded in the same mid-Middle Pleistocene redeposit (>240 ka) support recent conclusions that Chinese prehistory is much more complex than expected[19, 22, 24, 29, 49]. We identify three dental growth patterns with 1) two lineages of East Asian *Homo erectus*: PA 875 from very early Pleistocene populations (>2 Ma), TZ-1 is probably derived from a regional evolution; and 2) a more recent lineage from South Asian *Homo incertae sedis* (PA 874).

Acknowledgments: This work was supported by the Guizhou Engineering and Technology Research Center for Development and Utilization of Karst Cave Resources (G (2014) 4004) and the UMR 7194/CNRS-National Museum of Natural History, Paris, France. The authors express gratitude to Pr. Wu Xinzhi and to Dr. Cui Yaming for the pictures of the Tongzi teeth, to Pr. Zhao Lingxia for reception at the IVPP and for granting access to this collection and to Dr. Wu Xiujie for discussion and the pictures of Chaoxian and Changyang. The authors are grateful to Pr. Zhao Lingxia and Chen Xi for Chinese translations and to the anonymous reviewers for their fruitful remarks.

References

[1] Wu M, Wang L, Zhang Y, et al. Discovery of human fossils in association with lithic industry in Tongzi, Guizhou[J]. Vertebrata Palasiatica, 1975, 13(1): 14-23 (in Chinese)

[2] Zhang Y. The dental remains of early *Homo sapiens* found in China[J]. Acta Anthropologica Sinica, 1986, 5(2): 103-113

[3] Zhang Y, Liu W. Dental morphological distinctions between *Homo erectus* and early *Homo sapiens* in China[J]. Acta Anthropologica Sinica, 2002, 2(21): 87-101

[4] Zhang P, Dambricourt Malassé A, Cao Z, Lallouet F. Le potentiel paléoanthropologique et archéologique du karst de Yanhuidong (Tongzi), Province du Guizhou, Chine du sud[J]. Quaternaire, 2014, 25(3): 271-285

[5] Shen Q, Jin L. Uranium series datings of Yanhuidong, site of the man of Tongzi[J]. Acta Anthropologica Sinica, 1991, 10: 65-71 (in Chinese)

[6] Dambricourt Malassé A., Continuity and discontinuity during modalities of hominization[J]. In: Modes and Tempos in Evolution in the Quaternary, Quaternary Int., 1993, 19: 85-100

[7] Dambricourt Malassé, A. Evolution of the chondrocranium and the face from the Miocene anthropoids to *Homo sapiens*, continuities and discontinuities[J]. In: Climates, Cultures, Societies during Prehistoric Times. Palevol, 2006, 5: 109-117 (in French)

[8] Tillier A.M. Les dents d'enfant de Ternifine (Pléistocène moyen d'Algérie)[J]. L'Anthropologie, 1980, 84, 413–421

[9] Zanolli C, Bayle P, Macchiarelli R. Tissue proportions and enamel thickness distribution in the early Middle Pleistocene human deciduous molars from Tighenif, Algeria[J]. C. R. Palevol, 2010, 9: 341-348

[10] Bailey SE, Benazzi S, Souday C. Taxonomic differences in deciduous upper second molar crown outlines of *Homo sapiens*, *Homo neanderthalensis* and *Homo erectus*[J]. J Hum Evol, 2014, 72:1-9

[11] Kondo S, Wakatsuki E, Shun-Te H, et al. Comparison of the crown dimensions between the maxillary second deciduous molar and the first permanent molar[J]. Okajimas Folia Anat Jpn, 1996, 73(4):179-84

[12] Butler PM. Dental merism and tooth development[J]. J Dent Res, 1967, 46: 845-850

[13] Bailey SE. A morphometric analysis of maxillary molar crowns of Middle-Late Pleistocene hominins[J]. J Hum Evol, 2004, 4:183-198

[14] Martinón-Torres M, Bermúdez de Castro JM, Gómez-Robles A, et al. Dental remains from Dmanisi (Republic of Georgia): Morphological analysis and comparative study[J]. J Hum Evol, 2008, 55: 249-273

[15] Smith TM, Olejniczak A, Kupczik K, et al. Taxonomic assessment of the Trinil molars using non-destructive 3D structural and development analysis[J]. PaleoAnthropology, 2009, 117-129

[16] Bailey SE, Liu W. A comparative dental metrical and morphological analysis of a Middle Pleistocene hominin maxilla from Chaoxian (Chaohu), China[J]. Quatern Int, 2010, 211: 14-23

[17] Martinón-Torres M, Spěváčková P, Gracia-Téllez A, et al. Morphometric analysis of molars in a Middle Pleistocene population shows a mosaic of 'modern' and Neanderthal features[J]. J Anat, 2013, 223:353-363

[18] Liu W, Schepartz LA, Xing S et al. Late Middle Pleistocene hominin teeth from Panxian Dadong, South China[J]. J Hum Evol, 2013, 64: 337-355

[19] Zanolli C. Additional evidence for morpho-dimensional tooth crown variation in a new Indonesian H. erectus sample from the Sangiran Dome (Central Java)[J]. PLoS ONE, 2013, 8(7): e67233

[20] Zanolli C. Molar crown inner structural organization in Javanese *Homo erectus*[J]. Am J Phys Anthropol, 2015, 156(1): 148-157

[21] Xing S, Martinón-Torres M, Bermúdez de Castro JM, et al. Middle Pleistocene hominin teeth from Longtan Cave, Hexian, China[J]. PLoS ONE, 2014, 9(12): e114265

[22] Xing S, Martinón-Torres M, Bermúdez de Castro JM, et al. Hominin teeth from the early Late Pleistocene site of Xujiayao, Northern China[J]. Am J Phys Anthropol, 2015, 156(2): 224-240

[23] Xing S, Sun C, Martinón-Torres M, et al. Hominin teeth from the Middle Pleistocene site of Yiyuan, Eastern China[J]. J Hum Evol, 2016, 95: 33-54

[24] Martinón-Torres M, Xing S, Liu W, Bermudez de Castro JM. A "source and sink" model for East Asia? Preliminary approach through the dental evidence[J]. Palevol, 2016, DOI: 10.1016/j.crpv.2015.09.01

[25] Bailey, SE. The evolution of non-metric dental variation in Europe[J]. Mitteilungen der Gesellschaft für Urgeschichte, 2006, 15: 9-30

[26] Gómez-Robles A, Martinón-Torres M, Bermúdez de Castro JM, et al. A geometric morphometric analysis of hominin upper first molar shape[J]. J Hum Evol, 2007, 53: 272-285

[27] Quam R, Bailey SE, Wood BA. Evolution of M^1 crown size and cusp proportions in the genus *Homo*[J]. J Anat, 2009, 214: 655-670

[28] Liu W, Clarke R, Xing S. Geometric morphometric analysis of the early Pleistocene hominin teeth from Jianshi, Hubei Province, China[J]. Science China, Earth Sciences, 2010, 53(8): 1141-1152.

[29] Hao L, Chao Rong L, Kuman K. Longgudong, an Early Pleistocene site in Jianshi, South China, with stratigraphic association of human teeth and lithics[J]. Science China Earth, 2017, 60(3): 452-462

[30] Compton T, Stringer C. The morphological affinities of the Middle Pleistocene hominin teeth from Pontnewydd Cave, Wales[J]. J Quat Sc. 2015, 30: 713-730

[31] Palma di Cesnola A, Messeri M. P. Quatre dents humaines paléolithiques trouvées dans des cavernes de l'Italie Méridionale[J]. L'Anthropologie, 1967, 71: 249-262

[32] Sonika V, Harshminder K, Madhushankari GS. Sexual dimorphism in the permanent maxillary first molar: A study of the Haryana population (India)[J]. J Forensic Odontostomatol, 2011, 29: 37-43

[33] Wu M. New discovery of human fossils at Tongzi, Guizhou[J]. Acta Anthropologica Sinica, 1984, 3: 195-201 (in Chinese)

[34] Wu X, Poirier PE. Human Evolution in China: A Metric Description of the Fossils and a Review of the Sites[M]. Oxford University Press, Oxford, 1995: 317p

[35] Shen Q, Gao X, Gao B, et al. Age of Zhoukoudian *Homo erectus* determined with Al/Be burial dating[J]. Nature, 2009, 458: 198-200

[36] Molnar S. Human tooth wear, tooth function and cultural variability[J]. Am J Phys Anthropol, 1971, 34, 2: 175-189

[37] Wolpoff MH. The Krapina dental remains. American Journal of Physical Anthropology, 1979, 50: 67-114

[38] Wu XJ, Maddux SD, Pan L, et al. Nasal floor variation among eastern Eurasian Pleistocene *Homo*[J]. Anthropological Science, 2012, 120(3): 217-226

[39] Xiao D, Bae CJ, Shen G, et al. Metric and geometric morphometric analysis of new hominin fossils from Maba (Guangdong, China)[J]. J Hum Evol, 2014, 74: 1-20

[40] Kaifu Y, Kono RT, Sutikna T, et al. Unique dental morphology of *Homo floresiensis* and its evolutionary implications[J]. PLoS One, 2015, 10(11): e0141614

[41] Vallois HV, Thoma A. The teeth of Rabat Man[J]. Bull Mém Soc Anthropol Paris, 1977, 4(4): 31-58 (in French)

[42] Crevecoeur I, Skinner MM, Bailey SH, et al. First early hominin from Central Africa (Ishango, Democratic Republic of Congo)[J]. PLoS One, 2014, 9(1): e84652.

[43] Leakey MG, Spoor F, Dean MC. New fossils from Koobi Fora in northern Kenya confirm taxonomic diversity in early *Homo*[J]. Nature, 2012, 488: 201-204

[44] Brink JS, Herries AIR, Moggi-Cecchi J, et al. First hominine remains from a 1.0 million year old bone bed at Cornelia-Uitzoek, Free State Province, South Africa[J]. J Hum Evol, 2012, 63(3): 527-535

[45] Dirks PH, Roberts EM, Hilbert-Wolf H, et al. The age of *Homo naledi* and associated sediments in the Rising Star Cave, South Africa[J]. eLife, 2017, 6: e24231

[46] Berger, L, Hawks, J, de Ruiter DJ, et al. *Homo naledi*, a new species of the genus *Homo* from the Dinaledi Chamber, South Africa[J]. eLife, 2015, 4: e09560

[47] White TD, Asfaw B., De Gusta D et al. Pleistocene *Homo sapiens* from Middle Awash, Ethiopia[J]. Nature, 2003, 423: 742-747

[48] Shen G, Hua T, Xiao D, et al. Age of Maba hominin site in southern China: Evidence from U-series dating of Southern Branch Cave[J]. Quaternary Geochronology, 2014, 23: 56-62

[49] Liu W, Martinón-Torres M, Kaifu Y, et al. A mandible from the Middle Pleistocene Hexian site and its significance in relation to the variability of Asian *Homo erectus*[J]. Am J Phys Anthropol, 2017, 162(4): 715-731

[50] Ao H, Liu CR, Roberts AP, et al. An updated age for the Xujiayao hominin from the Nihewan Basin, North China: Implications for Middle Pleistocene human evolution in East Asia[J]. J Hum Evol, 2017,106: 54-65

[51] Liu W, Martinón-Torres M, Cai YJ, et al. The earliest unequivocally modern humans in southern China[J]. Nature, 2015, 526: 696-699

[52] Michel V, Valladas H, Shen G, et al. The earliest modern *Homo sapiens* in China?[J]. J Hum Evol, 2016, 101: 101-104

[53] Zaim Y, Ciochon RL, Polanski JM. New 1.5 million-year-old *Homo erectus* maxilla from Sangiran (Central Java, Indonesia)[J]. J Hum Evol, 2011, 376(4): 363

[54] Richter D, Grün R, Joannes-Boyau R, et al., The age of the hominin fossils from Jebel Irhoud, Morocco, and the origins of the Middle Stone Age[J]. Nature, 2017, 546: 293-296

[55] Hublin JJ, Ben-Ncer A, Bailey SE, et al. New fossils from Jebel Irhoud, Morocco and the pan-African origin of *Homo sapiens*[J]. Nature, 2017, 546: 289-292